SEMARAK ILMU PUBLISHING

Journal of Advanced Research in Applied Mechanics

Journal homepage:
https://semarakilmu.com.my/journals/index.php/appl_mech/index
ISSN: 2289-7895

Radiation and Nanoparticles Shape Effect on Aligned MHD Jeffrey Hybrid Nanofluids Flow and Heat Transfer over a Stretching Inclined Plate

Mohd Rijal Ilias[1], Nurul Nabilah Rosli[1], Siti Shuhada Ishak[1], Vincent Daniel David[1,*], Sharidan Shafie[2], Mohd Nashriq Abd Rahman[3]

[1] School of Mathematical Sciences, College of Computing, Informatics and Media, Universiti Teknologi MARA, 40450 Shah Alam, Selangor, Malaysia
[2] Department of Mathematical Sciences, Faculty of Science, Universiti Teknologi Malaysia, 81310 Johor Bahru, Johor, Malaysia
[3] Jabatan Meteorologi Malaysia, Jalan Sultan, 46667 Petaling Jaya, Selangor, Malaysia

ARTICLE INFO

Article history:
Received 28 May 2023
Received in revised form 31 July 2023
Accepted 12 August 2023
Available online 21 August 2023

Keywords:
Jeffrey hybrid nanofluids; radiation; aligned MHD; nanoparticles shape; stretching inclined plate

ABSTRACT

The study through a stretching medium is a topic in the field of fluid dynamics and heat transfer. It involves investigating the behaviour of fluid flow and heat transfer phenomena in situations where a medium, such as a solid surface, is continuously stretched or deformed. Jeffrey fluid are found in the applications in various fields, including engineering, materials science, and biomedical engineering. Water was combined with copper (Cu) and aluminium oxide (Al_2O_3) is used in this study by considering the influence of nanoparticles shape which are spherical, brick, cylindrical, platelet and blade. The Keller Box method is used to solve numerically the Jeffrey hybrid nanofluid's governing nonlinear partial differential equations (PDEs) to nonlinear ordinary differential equations (ODEs) using similarity transformation. The results for both the velocity and temperature profiles of Jeffrey hybrid nanofluids (Deborah number, β) as well as the skin friction and Nusselt number are presented graphically and in tabulated form. The result shows that the momentum boundary layer thickness is decrease for any increment of the value alignment angle of the magnetic field parameter, the interaction of the magnetic field parameter, alignment angle of the incline plate, the mixed convection parameter, the radiation parameter, and the nanoparticles shape except the value of the volume fraction of the nanoparticles for the increasing value of Deborah number (β). The skin friction is increases as any increment value of an alignment angle of magnetic field, interaction of magnetic parameter, radiation parameter and volume fraction of nanoparticles increase, while the Nusselt number is decrease for the value of radiation parameter. It also observed that the factor of nanoparticles shape result is significant with the Jeffrey hybrid nanofluids which is the nanoparticles shape with the highest skin friction coefficient and Nusselt number is blades shape.

* *Corresponding author.*
E-mail address: vincent@fskm.uitm.edu.my

https://doi.org/10.37934/aram.109.1.84102

1. Introduction

Nanotechnology has advanced significantly over the past few decades and set the foundation for some very astounding industrial applications. It involves the design, fabrication, and application of materials and devices with unique properties and functionalities at the nanometer scale (typically ranging from 1 to 100 nanometers) [1]. In the field of heat transfer, nanofluids is an approach to improve heat transfer efficiency and thermal management. According to Choi's theory [2], nanofluids is consist of nanoparticles dispersed in a base fluid. Then, there are a relatively new type of nanofluids that can be made by suspending two or more types of nanoparticles in a base fluid known as a hybrid nanofluids. The idea of using hybrid nanofluids is to balance the benefits and disadvantages of separate suspensions, hybrid nanofluids create considerable changes in heat transfer and pressure drop requirements, which can be attributed to a higher aspect ratio, a more suited thermal network, and the synergistic effect of nanoparticles [3]. This is proven by Waini *et al.,* [4] analyzed a hybrid nanofluid's steady flow and heat transfer was found the heat transfer rate of hybrid nanofluids to be higher than nanofluids. Idris *et al.,* [5] proposed the idea of using hybrid nanofluid is to improve thermal properties compared to base fluids and mono nanofluid due to the synergistic effect. The study on hybrid nanofluids was discovered in different situation by some researchers [6-7].

A Jeffrey fluid is a non-Newtonian fluid that exhibits viscoelastic behavior which display a time-dependent response to applied shear. When nanoparticles are dispersed in a Jeffrey fluid, it forms a Jeffrey hybrid nanofluids [8]. The impact of various factors, including nanoparticle concentration, size, material, and dispersion quality, on the thermal conductivity of the Jeffrey hybrid nanofluids can optimize the thermal conductivity enhancement for improved heat transfer performance. Jeffrey hybrid nanofluids performance of thermal systems has been used in various industries, including electronics cooling, energy conversion, and thermal management applications. The impact of applied magnetohydrodynamics (MHD) and radiation on Jeffrey hybrid nanofluids can affects the heat transfer characteristics. Study by Zokri *et al.,* [9] on the influence of the radiation on MHD flow and heat transfer of a Jeffrey fluid over a stretching sheet found that the velocity is increase for any an increment in Jeffrey fluid parameter while the temperature id decrease. Rawi *et al.,* [10] studied unsteady mixed convection flow of Jeffrey fluid past an inclined stretching sheet with the presence of nanoparticles and found that the effect of Jeffrey fluid parameter and ratio of relaxation to retardation times give a significant effect on the variation of skin friction and heat transfer coefficients with the present of g-jitter. Shahzad *et al.,* [11] conducted a study on the effects on MHD heat transfer flow of Jeffrey nanofluids and found that the temperature is improve by increase the value of magnetic parameter. The study on magnetic field flow by Ali *et al.,* [12] of Jeffrey in hybrid nanofluids was found that the rise in values of Jeffrey parameters leads to a temperature decrement while an enhancement in volume friction of nanoparticles reduces both temperature and velocity. The effect of magnetic force on Jeffrey hybrid nanofluids by Alqarni *et al.,* [13] also found the induced magnetic field and temperature are significant under the variation parameters of the problem. The study of hydromagnetic on non-Newtonian fluids with dual effect features is viscoelastic fluid with effect of and radiation by Jafar *et al.,* [14]. They found that the impact of the applied magnetic parameter is improve the distribution of the viscoelastic fluid temperature and reduce the temperature gradient at the border. Also, an increase in temperature distribution and the associated thermal layer is caused by radiation.

The study on the topic of MHD and radiation has developed quickly by considering the different problems and situations. Ilias *et al.,* [15] studied the heat transfer rate of an MHD flow and found that, for the case of unsteady and steady fluid flow, an increase in nanoparticles volume fraction and magnetic field strength elevates the Nusselt number. Nayan *et al.,* [16] studied an aligned (MHD)

flow of hybrid nanofluids by using a Keller Box method and found that when the angle of aligned magnetic field and the interaction of magnetic parameter increase show that the velocity profiles increase while temperature profiles decrease. Zainal *et al.,* [17] investigated the steady MHD of a hybrid nanofluids and revealed that as the magnetic parameter's value grows, the fluid velocity increases but the fluid temperature decreases, which is counterintuitive. Bosli *et al.,* [18] study the effect on magnetic nanoparticle with different base fluids past and found that the magnetic field has a significant effect on the fluid flow and heat transfer characteristics of the system. Yashkun *et al.,* [19] examine the heat transfer characteristic of the (MHD) hybrid nanofluids over the linear stretching and shrinking surface in the presence of thermal radiation effects and found that the values of the skin friction coefficient increase, but the local Nusselt number decreases with the increasing of thermal radiation parameter. Other researchers were discussing in [20-33].

The shape of nanoparticles influences the effective thermal conductivity and convective heat transfer coefficient of the nanofluids. Nanoparticle shape refers to the geometry or morphology of nanoparticles dispersed in the nanofluids. The shape of nanoparticles can vary, including spherical, cylindrical, plate-like, or irregular shapes. The effects of nanoparticle shapes on flow and heat transfer properties in both laminar and turbulent flow regimes serve as the driving force was study by Shahsavar *et al.,* [34]. It shown that the shape of the used nanoparticles plays a significant role in these differences in the parameters, with platelet-shaped particles being the most favourable. Other than that, Hemalatha *et al.,* [35] study the mixed convective flow considering the effect of the shapes of the nanoparticles and shows that the temperature distribution is increase noticed with the spherical shaped particles, as the nanoparticle volume fraction increases in the base fluid. Khetib *et al.,* [36] examined the turbulent flow that contains platelet, brick, blade, and cylinder-shaped nanoparticles. The studied of aligned MHD natural convection flow and heat transfer considering the nanoparticles shape factor by Bosli *et al.,* [18] was found that the nanoparticles shape of laminar has the highest velocity and temperature while the spherical shape has the lowest for all parameters.

However, the combination of radiation, aligned MHD effects, and nanoparticle shape in Jeffrey hybrid nanofluids flow and heat transfer over a stretching inclined plate leads to a complex interplay between various heat transfer mechanisms. Hence, a study was conducted to understand the influenced of water was combined with copper (Cu) and aluminium oxide (Al_2O_3) by considering spherical, brick, cylindrical, platelet and blade shape nanoparticles as a shape factor is studied.

2. Mathematical Formulation

Formulation and diagram for the problem of this research has been explained under this section. This research considered a continuous, incompressible two-dimensional MHD Jeffrey hybrid nanofluids over a stretching inclined plate with constant wall temperature as shown in Figure 1. The stretching velocity is $u_w(x) = cx$ in which stretching and shrinking constant variable is denoted by $c > 0$ and $c < 0$ respectively, whereas $u_e(x) = ax$ remark as the velocity of ambient fluid. In addition, the plate does not move when $c = 0$. The ambient fluid temperature is assumed to be uniform, T_∞ and T_w is constant wall temperature.

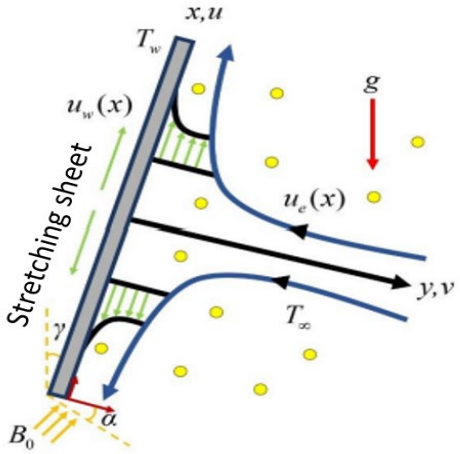

Fig. 1. Physical Model of Stretching Inclined Plate

A magnetic force was applied to the flow with angle of acute. The function for the distance from origin was identified as $B(x) = \frac{B_0}{\sqrt{x}}$, B_0 is the strength of magnetic field and x is the coordinate along the plate. As soon as the magnetic field is applied, the nanoparticles were oriented quickly along the magnetic field lines. The particles are randomized easily after the magnetic field is removed. The hybrid nanofluids is a composed of Water based Cu-Al_2O_3 nanoparticles. The base fluid and the suspended nanoparticles are assumed to be in thermal equilibrium. The continuity, momentum and energy equation were the main three equations in this study. The flow within the laminar boundary layer was assumed to be a two-dimensional and steady. [7, 9, 10].

$$\frac{\partial u}{\partial x} + \frac{\partial v}{\partial y} = 0 \tag{1}$$

$$u\frac{\partial u}{\partial x} + v\frac{\partial u}{\partial y} = \frac{\mu_{hnf}}{\rho_{hnf}(1+\lambda_1)}\left(\frac{\partial^2 u}{\partial y^2} + \lambda_2\left(u\frac{\partial^3 u}{\partial x \partial y^2} + \frac{\partial u}{\partial y}\frac{\partial^2 u}{\partial x \partial y^2} + v\frac{\partial^3 u}{\partial x \partial y^2} - \frac{\partial u}{\partial x}\frac{\partial^2 u}{\partial y^2}\right)\right) + \frac{\sigma B_0^2}{\rho_{nf}} sin^2\alpha(u) + \frac{(\rho\beta)_{nf}}{\rho_{nf}} g(T - T_\infty) g\cos\gamma(T - T_\infty) \tag{2}$$

$$u\frac{\partial T}{\partial x} + v\frac{\partial T}{\partial y} = \frac{k_{hnf}}{(\rho C_p)_{hnf}}\frac{\partial^2 T}{\partial y^2} - \frac{1}{(\rho C_p)_{hnf}}\frac{\partial q_r}{\partial y} \tag{3}$$

While the boundary conditions used in this study are as follows:

$$\begin{aligned} &u = U_w(x), \quad v = 0, \quad T = T_w && on\ y = 0 \\ &u \to 0, \quad T \to T_\infty && as\ y \to \infty \end{aligned} \tag{4}$$

where u and v are denoted as component of velocity in x and y directions, respectively. α is the aligned angle of magnetic field, T is the fluid temperature, g is the acceleration due to gravity, ρ_{hnf} and $(\rho\beta)_{hnf}$ are the effective density and thermal expansion coefficient of hybrid nanofluids, σ is the electrical conductivity, μ_{hnf} is the effective dynamic viscosity of hybrid nanofluids, $(\rho C_p)_{hnf}$ is

the heat capacity of the hybrid nanofluids, k_{hnf} is the thermal conductivity of the hybrid nanofluids, λ_1 is the ratio of relaxation to retardation times, λ_2 is the retardation time, M is magnetic parameter and γ is the plate inclination angle parameter. The Rosseland approximation for radiation [37] is utilized, hence,

$$q_r = -\frac{4\sigma^*}{3k^*}\frac{\partial T^4}{\partial y} \tag{5}$$

where σ^* is the Stefan Boltzmann whereas and k^* is the mean absorption coefficients. Next, Taylor's series is extended to the temperature difference in the flow. By extending T^4 over T_∞ with the higher-order terms is being neglected, therefore,

$$T^4 \cong 4T_\infty^3 T - 3T_\infty^4 \tag{6}$$

Table 1 demonstrates the thermophysical relation of hybrid nanofluids where ϕ_1 and ϕ_2 are the solid volume fraction of nanoparticles Cu and Al_2O_3 respectively. ρ_f and ρ_s are the densities of base fluid and solid particles where ρ_{s1} is the effective density of Cu while ρ_{s2} is the effective density of Al_2O_3. $(C_p)_f$ and $(C_p)_s$ is the heat capacity of the fluid and solid particles which $(C_p)_{s1}$ as the heat capacity of the Cu and $(C_p)_{s2}$ is the heat capacity of the Al_2O_3. μ_f is the dynamic viscosity of fluid, k_f is the thermal conductivity of the fluid, k_{s1} is the thermal conductivity of Cu, k_{s2} is the thermal conductivity of Al_2O_3. The shape factor is represented as m, β_f and β_s are the thermal expansion coefficients of the base fluid and nanoparticles, respectively where β_f is the thermal expansion coefficient of Cu and β_{s2} is the thermal expansion coefficient of Al_2O_3.

Table 2 displays the thermophysical properties of base fluid, which is Water and nanoparticles, taken from research by Zainal *et al.,* [17] and Waini *et al.,* [4]. Copper (Cu) and aluminium oxide (Al_2O_3) are the nanoparticles that will be employed in this current study. To solve the governing equation in Eq. (1)-(3), the following similarity variable are introduced,

Table 1
Thermophysical Relation of Hybrid Nanofluids [18]

Properties	Hybrid Nanofluids	
Density	$\rho_{hnf} = (1-\phi_2)\left[(1-\phi_1)\rho_f + \phi_1\rho_{s1}\right] + \phi_2\rho_{s2}$	(7)
Heat Capacity	$(\rho C_p)_{hnf} = (1-\phi_2)\left[(1-\phi_1)(\rho C_p)_f + \phi_1(\rho C_p)_{s1}\right] + \phi_2(\rho C_p)_{s2}$	(8)
Viscosity	$\mu_{hnf} = \dfrac{\mu_f}{(1-\phi_1)^{2.5}(1-\phi_2)^{2.5}}$	(9)
Thermal Conductivity	$\dfrac{k_{hnf}}{k_{bf}} = \dfrac{k_{s2} + (m-1)k_{bf} - (m-1)\phi_2(k_{bf} - k_{s2})}{k_{s2} + (m-1)k_{bf} + \phi_2(k_{bf} - k_{s2})}$	(10)
	$\dfrac{k_{bf}}{k_f} = \dfrac{k_{s1} + (m-1)k_f - (m-1)\phi_1(k_f - k_{s1})}{k_{s1} + (m-1)k_f + \phi_1(k_f - k_{s1})}$	
	$k_{bf} = \dfrac{k_{s1} + (m-1)k_f - (m-1)\phi_1(k_f - k_{s1})}{k_{s1} + (m-1)k_f + \phi_1(k_f - k_{s1})} \times k_f$	
	$\dfrac{k_{hnf}}{k_f} = \dfrac{k_{hnf}}{k_{bf}} \times \dfrac{k_{bf}}{k_f}$ $= \dfrac{k_{s2} + (m-1)k_{bf} - (m-1)\phi_2(k_{bf} - k_{s2})}{k_{s2} + (m-1)k_{bf} + \phi_2(k_{bf} - k_{s2})} \times$ $\dfrac{k_{s1} + (m-1)k_f - (m-1)\phi_1(k_f - k_{s1})}{k_{s1} + (m-1)k_f + \phi_1(k_f - k_{s1})}$	
	where	
	$\dfrac{k_{bf}}{k_f} = \dfrac{k_{s1} + (m-1)k_f - (m-1)\phi_1(k_f - k_{s1})}{k_{s1} + (m-1)k_f + \phi_1(k_f - k_{s1})}$	(11)
Thermal Expansion Coefficient	$\beta_{hnf} = (1-\phi_2)\left[(1-\phi_1)\beta_f + \phi_1\beta_{s1}\right] + \phi_2\beta_{s2}$	(12)
	$(\rho\beta)_{hnf} = (1-\phi_2)\left[(1-\phi_1)(\rho\beta)_f + \phi_1(\rho\beta)_{s1}\right] + \phi_2(\rho\beta)_{s2}$	(13)
Thermal Diffusivity	$\alpha_{hnf} = \dfrac{k_{hnf}}{(\rho C_p)_{hnf}}$	(14)

Table 2
Thermophysical Properties of Copper and Aluminium Oxide Nanoparticles and Water Based Fluid [4, 17].

Physical Properties	Cu	Al_2O_3	Base fluid (Water)
$\boldsymbol{\rho(kg/m^3)}$	8933	3970	997.1
$\boldsymbol{C_p(J/kgK)}$	385	765	4179
$\boldsymbol{k(W/mK)}$	400	40	0.613
$\boldsymbol{\beta \times 10^{-5}(K^{-1})}$	1.67	0.85	21
Pr	6.2		

$$\eta = y\sqrt{\frac{c}{v_f}}, \qquad \psi = \sqrt{cv_f}xf(\eta), \qquad \theta = \frac{T - T_\infty}{T_w - T_\infty} \tag{15}$$

where $Re_x = \frac{U_w x}{v_f}$ is the Reynolds number and ψ is a stream function of the form in which related to *u* and *v* as below:

$$u = \frac{\partial \psi}{\partial y}, v = -\frac{\partial \psi}{\partial x} \tag{16}$$

By substituting Eq. (7)-(14), (15), (16) into Eq. (2) and Eq. (3), the following nonlinear ODEs of momentum and energy are obtained:

$$\begin{aligned} &f'''(\eta) + \kappa\left(\left(f''(\eta)\right)^2 - f(\eta)f^{IV}(\eta)\right) - A_1(1+\lambda_1)Mf'(\eta)\sin^2\alpha \\ &+A_1A_3(1+\lambda_1)\lambda\theta(\eta) + A_1A_2(1+\lambda_1)\left[f(\eta)f''(\eta) - \left(f'(\eta)\right)^2\right] \end{aligned} \tag{17}$$

$$\frac{1}{Pr}A_4\left[A_4 + \frac{4}{3}Rd\right]\theta''(\eta) - f(\eta)\theta'(\eta) = 0 \tag{18}$$

The boundary condition derived by applying (4) are as follows:

$$\begin{aligned} &f(0) = 0, \ f'(0) = 1, \ \theta(0) = 1 && on \ \eta = 0 \\ &f'(\eta) = 1, \ \theta(\eta) = 0, && \text{as } \eta \to \infty \end{aligned} \tag{19}$$

Numerical findings are discussed using the skin friction coefficient at the plate's surface and the local Nusselt number, which are specified as:

$$C_f = \frac{\tau_w}{\rho_f {U_\infty}^2}, \quad Nu_x = \frac{xq_w}{k_f\left(T_f - T_\infty\right)} \tag{20}$$

$$\tau_w = \mu_{nf}\left(\frac{\partial u}{\partial y}\right)_{y=0}, \qquad q_w = -k_{nf}\left(\frac{\partial T}{\partial y}\right)_{y=0} + \left(\frac{\partial q}{\partial r}\right)_{y=0} \tag{21}$$

where τ_w is the wall skin friction (shear stress) and q_w is the plate's constant heat flux. By substituting (16) and (21) into (20), the solutions obtained are as follows:

$$(Re_x)^{\frac{1}{2}}C_f = \frac{1}{(1-\phi_1)^{2.5}(1-\phi_2)^{2.5}} f''(0), \quad \frac{Nu_x}{(Re_x)^{\frac{1}{2}}} = -\left[\frac{k_{nf}}{k_f} + \frac{4}{3}Rd\right]\theta'(0) \tag{22}$$

where,

$$A_1 = (1-\phi_1)^{2.5}(1-\phi_2)^{2.5}, \quad A_2 = (1-\phi_2)\left\{(1-\phi_1) + \phi_1\frac{\rho_{s1}}{\rho_f}\right\} + \phi_2\frac{\rho_{s2}}{\rho_f},$$

$$A_3 = (1-\phi_2)\left\{(1-\phi_1) + \phi_1\frac{(\rho\beta)_{s1}}{(\rho\beta)_f}\right\} + \phi_2\frac{(\rho\beta)_{s2}}{(\rho\beta)_f}, \quad A_4 = \frac{(\rho C_p)_f}{(\rho C_p)_{hnf}}$$

$$A_5 = \frac{k_{hnf}}{k_f}, \quad Rd = \frac{4T_\infty^3\sigma^*}{k_f k^*}, \quad M = \frac{\sigma {B_0}^2}{c\rho_f},$$

$$\lambda = \frac{Gr_x}{{Re_x}^2}, \quad Pr = \frac{\upsilon_f}{\alpha_f}, \quad \kappa = c\lambda_2, \quad Gr_x = \frac{g\beta_f(T_w - T_\infty)x^3}{{\upsilon_f}^2}$$

3. Numerical Solution

The Keller Box method is an implicit finite-difference method in conjunction with Newton's method for linearization. The nonlinear system of differential Eq. (17) and (18) subject to boundary conditions Eq. (19) are solved numerically using the Keller-box method with Fortran Programming software. The previous studies which use the Keller-box method in solving boundary layer problems including Ishak *et al.,* [38, 39], Ilias *et al.,* [15, 26], Rawi *et al.,* [10]. As mentioned in the books by Na [40] and Cebeci and Bradshaw [41], the Keller-box method consists of four main steps:

i. Reduce the differential Eq. (2) and Eq. (3) to first order equations as Eq. (17) and Eq. (18),
ii. Write the difference equation using central differences,
iii. Linearize the resulting algebraic equations by Newton's method and write them in the matrix-vector form,
iv. Solve the linear system by the block tri-diagonal elimination technique.

The results of the current study were compared to the results of a previous study to validate the validity and correctness of the present analysis. Table 3 and 4 shows the comparison values with previous published results reported by Das *et al.,* [42], Ulgen *et al.,* [43] and Ishak *et al.,* [38]. It is seen that the present values $C_f Re_x^{\frac{1}{2}}$, are in very good agreement in Table 3 while Table 4 is comparison between values of $C_f Re_x^{\frac{1}{2}}$ and $Nu_x Re_x^{-\frac{1}{2}}$.

Table 3

Comparison results for the values of $C_f Re_x^{\frac{1}{2}}$ for different values a/c when the buoyancy term λ is absent

a/c	Das *et al.,* [42]	Ulgen *et al.,* [43]	Ishak *et al.,* [38]	Present
0.1	-0.9694	-0.9694	-0.9694	-0.9694
0.2	-0.9181	-0.9181	-0.9181	-0.9181
0.5	-0.6673	-0.6673	-0.6673	-0.6673
2	2.0175	2.0176	2.0176	2.0176
3	4.7293	4.7296	4.7294	4.7293

Table 4

Comparison results for the values of $C_f Re_x^{\frac{1}{2}}$ and $Nu_x Re_x^{-\frac{1}{2}}$ for $a/c = 1, \lambda = 1$ and different values of Pr

Pr	Buoyancy assisting flow			
	Ishak *et al.,* [38]		Present	
	$C_f Re_x^{\frac{1}{2}}$	$Nu_x Re_x^{-\frac{1}{2}}$	$C_f Re_x^{\frac{1}{2}}$	$Nu_x Re_x^{-\frac{1}{2}}$
0.72	0.3645	1.0931	0.3645	1.0931
6.8	0.1804	3.2902	0.1804	3.2466
20	0.1175	5.6230	0.1175	5.6201
40	0.0873	7.9463	0.0872	7.9383

4. Results and Discussion

The governing boundary layer Eq. (2) and (3) with boundary condition [4] were numerically solved by using Keller-Box Method and was coded using the MATLAB software for this study's results. The influence of the alignment angle of the magnetic field parameter (α), the interaction of the magnetic field parameter (M), alignment angle of the incline plate (γ), the mixed convection parameter (λ), the radiation parameter (Rd), the volume fraction of the nanoparticles $(\phi_1 \; and \; \phi_2)$, are graphically presented in Figure 2-7. The skin friction coefficient and Nusselt number for different Deborah number (β) are recorded in the Table 5. While skin friction coefficient and Nusselt number for different of nanoparticle shape are display in the Table 6.

The results of different variations of flow parameters are presented and discussed as below. The thermophysical properties of the nanoparticles and base fluid are given in Table 2. The parameters used for simulation are $\alpha = 90^{\circ}, \mathrm{M} = 1, \gamma = 45^{\circ}, \mathrm{Rd} = 1, \lambda = 0.02, \phi_1 = 0.1 \text{ and } \phi_2 = 0$ and $\beta = 0.5, 1 \text{ and } 1.5$, unless otherwise stated:

Figure 2(a) and (b) illustrates the influence of different values of inclination angle of magnetic field, α on the velocity and temperature. From Figure 2(a), it is observed that the increment in α causes the velocity profiles is decrease. An increment in α also causes the boundary layer thickness to decrease. Other than that, velocity is noticeably decrease for the rising β and the thickness of momentum boundary layer to decrease. The increase of the aligned angle makes the magnetic field becomes stronger thus pushes the Jeffrey hybrid nanofluids towards the plate. When $\alpha = 0°$, it indicates that there is no magnetic field but when $\alpha = 90°$, the aligned magnetic field behaves like a transverse magnetic field and due to changes in the position of the aligned magnetic field, it attracts the nanoparticles. From Figure 2(b) it is depicted that an increase in α and β lead to the increment in temperature profiles. Besides, thermal boundary layer thickness also increases. It is also shows that when the magnetic field is added to a magnetic fluid flow, the heat transfer coefficient where the α exists is significantly higher than the heat transfer coefficient under no magnetic field. As the α increases, the heat transfer enhances.

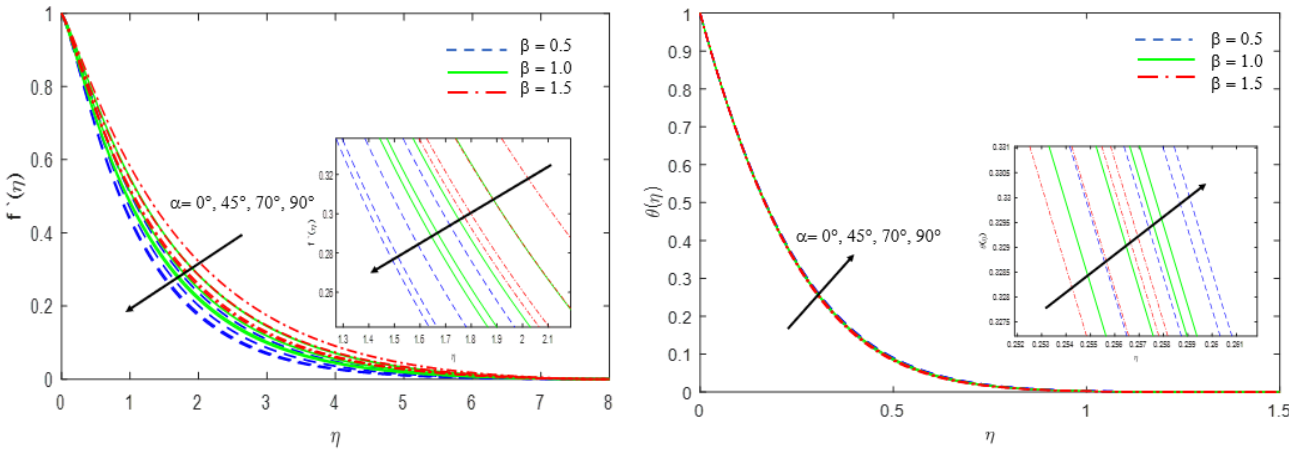

(a) (b)

Fig. 2. Effects of inclination angle of magnetic field, α on (a) velocity (b) temperature

Figure 3 (a) and (b) shows the effects of various magnetic parameter, M on velocity profiles. From Figure 4, when M increases, the velocity profiles decrease due to the inflection of the vertical magnetic field to the electrically conducting fluid the Lorentz force is produced. This force has the tendency to slow down the flow and as a result the velocity profile decreases. Momentum boundary layer thickness is decrease in M while β is increases. When $M = 0$, there is no magnetic force present and when the strength of the magnetic field increases, the fluid is pushed towards the plate thus the momentum boundary layer is reduced. The increasing in M leads to generate the Lorentz force, in which it gives conflict to flow and cuts down the velocity of fluid. The effect of parameter M on the temperature profiles is demonstrated in Figure 3 (b). When M rises, the temperature profiles across the plate increase, alongside with the thermal boundary layer thickness. Physically, the Lorentz force due to the transverse magnetic field has the property of relaxing the fluid temperature distributions [38]. It is also shows as the β is increases, the boundary layer thickness also increases.

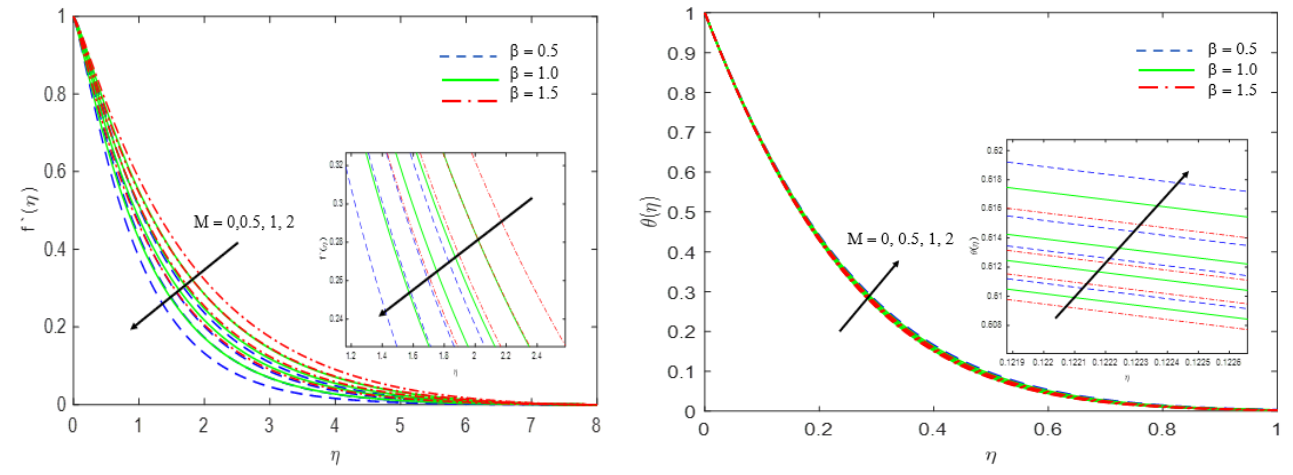

(a) (b)

Fig. 3. Effects of inclination angle of magnetic field, M on (a) velocity (b) temperature

Figure 4 (a) and (b) shows the impact of different inclination angle of plate, γ on velocity and temperature profiles. In Figure 4 (a), the increase in γ causes the velocity profiles to increase and the momentum boundary layer thickness to rise. The plate is assumed to be in a vertical and horizontal position when $\gamma = 0°$ and $\gamma = 90°$, respectively, meanwhile the plate is in a slanted position when

$\gamma = 40°$ and $\gamma = 70°$. Other than that, the figure shows that momentum boundary layer thickness decreases as β is increases. It can be observed that from Figure 4 (b), an increase in γ decreases the temperature profiles and the thermal boundary layer. This is because a stronger force is required by the fluid to flow better thus affects the temperature. Next, the momentum boundary layer thickness increases as β is increases from 0.5 to 1.5.

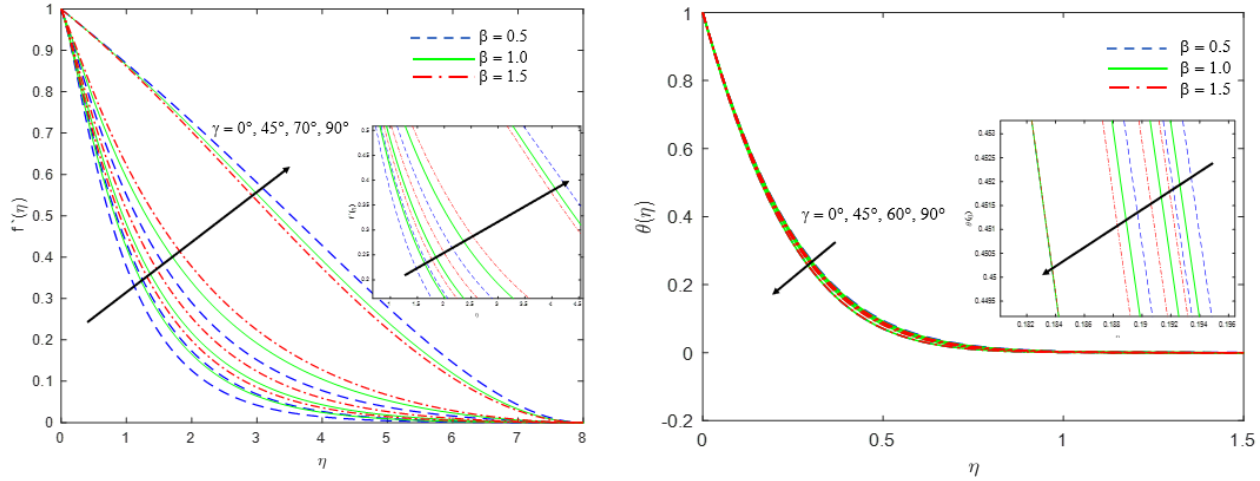

(a) (b)

Fig. 4. Effects of inclination angle of magnetic field, γ on (a) velocity (b) temperature

The influence of different values of the mixed convection parameter, λ on the velocity and temperature profile is shown in Figure 5 (a) and (b). As seen in the Figure 5 (a), the velocity profiles increase with increasing λ values while the momentum boundary layer decreases. This happens due to the larger values of buoyancy force. If the value of the mixed convection parameter is magnified, therefore the buoyancy will increase. Hence, the flow velocity increases as the buoyancy grows. The effect of β is also shown in Figure 5 (a). As the β increases, the momentum boundary layer thickness also increases. It can be seen from Figure 5 (b), when there is an increase in λ, the temperature profiles and the thermal boundary layer will shrink. This is due to the increasing in the convection cooling effect as λ increase thus the temperature is reduced. Other than that, the boundary layer thickness of rising β is also decreasing.

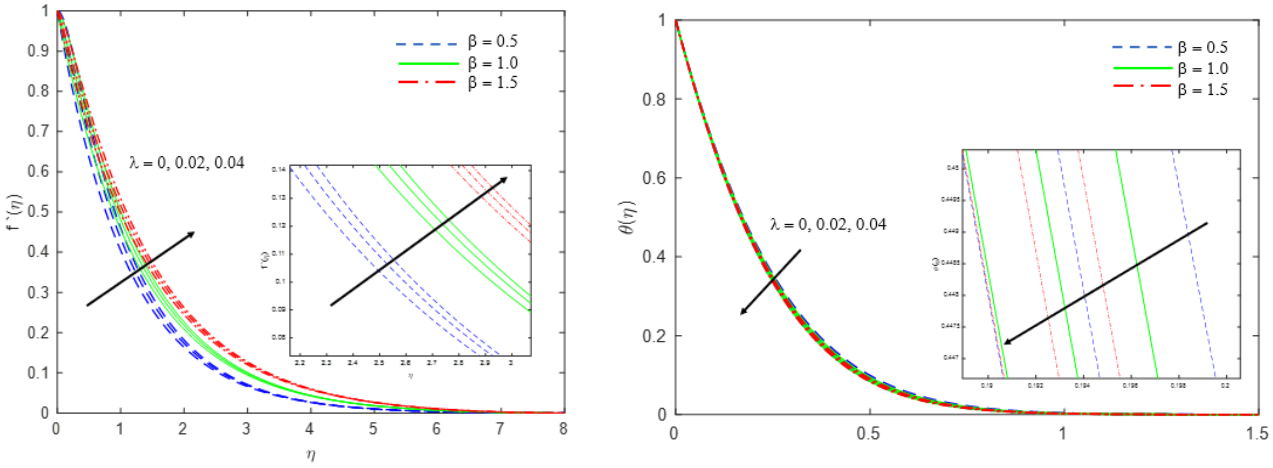

(a) (b)

Fig. 5. Effects of inclination angle of magnetic field, λ on (a) velocity (b) temperature

Figure 6 (a) and (b) exhibits the effect of the Rd on the velocity and temperature profiles. It shows that the velocity of fluid enhances with the increase in the parameter value of Rd in Figure 6 (a). However, for the momentum boundary layer thickness, it is decreasing as the Rd increases. For β is increases, the momentum boundary layer thickness also increases. Meanwhile Figure 6 (b) exhibits the effect of the Rd on the temperature profiles. It shows that the temperature of fluid enhances with the increase in the parameter value of Rd. The reason behind this behaviour is that Rosseland, the means absorption coefficient is increases when Rd rises. This led to an increase of large heat quantity to improve the values of Rd. The momentum boundary layer thickness is decreasing for increasing Rd. The β is increases cause momentum boundary layer thickness also increases.

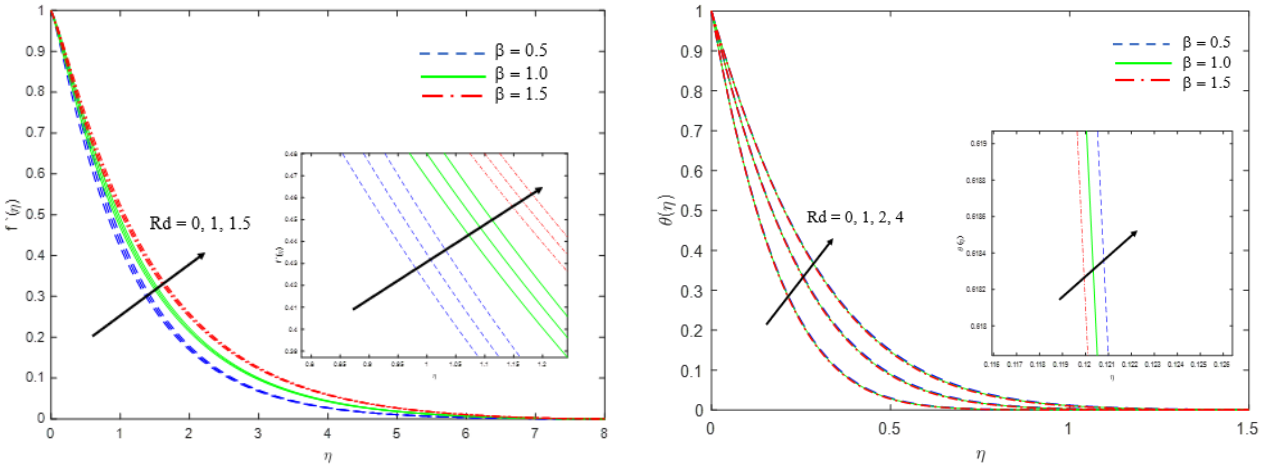

(a) (b)

Fig. 6. Effects of inclination angle of magnetic field, Rd on (a) velocity (b) temperature

Figure 7 (a) and 7 (b) shows the impact of varying nanoparticles volume fractions on velocity and temperature profiles for the inclined plate. In Figure 7 (a), the velocity profile increases due to the growth of $\phi_1 \text{and } \phi_2$, and the thickness of the momentum boundary layer increases. Since viscosity is the resistance to flow in a fluid, thus the lower the viscosity, the more readily the fluid flows, which causes the velocity to increase. Other than that, as the value of β is increased, it is observed that velocity profiles are increased as well as momentum boundary layer thickness. This shows that the velocity of the fluid increases inside the boundary layer. The temperature profiles in Figure 7 (b) increase when $\phi_1 \text{and } \phi_2$ increase. This is due to the increases in the rate of heat transportation and more energy is physically dispersed when the nanoparticles volume fraction is increased, thus raising the temperature consequently. Additionally, the thermal boundary layer thickness is also enhanced by the influence of the increment in $\phi_1 \text{and } \phi_2$. In the case of temperature profile as the β is increased the temperature slightly boosts. However, it is noticed the β does not have much effect on the temperature at some distance from the surface inside the thermal boundary layer.

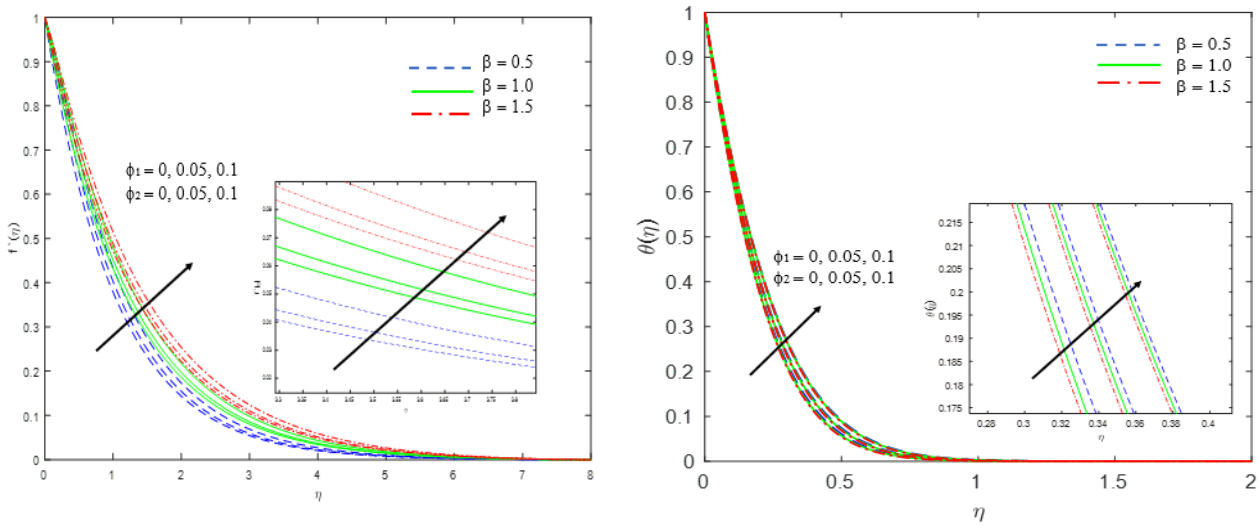

(a) (b)

Fig. 7. Effects of inclination angle of magnetic field, $\phi_1 and\ \phi_2$ on (a) velocity (b) temperature

As displayed in Table 5, for the value of $\beta = 0.5$, $\beta = 1$ and $\beta = 1.5$, as the $\gamma, \lambda, Rd, \phi_1\ and\ \phi_2$ increases the skin friction is decreases, while as increases the value of α and M the skin friction is increase since different degrees of stretching plate noticeably affect the rate of heat transfer skin friction coefficient. For Nusselt number, it shows that as increase in α, M, ϕ_1 and ϕ_2, the Nusselt number is increases, while the Nusselt number is decreases for an increment in $\gamma, Rd\ and\ \lambda$. The Nusselt number can be negative since it is defined as the dimensionless temperature gradient at the wall. It also shows that, as the value of $\alpha, \gamma, \lambda, Rd, \phi_1\ and\ \phi_2$, the lowest skin friction coefficient is $\beta = 1.5$ compared to other. As a value of $\lambda, Rd, \phi_1\ and\ \phi_2$, the highest Nusselt number is $\beta = 0.5$ while for the value of α shows that the highest Nusselt number is $\beta = 1$ and $\beta = 1.5$ for γ compared to others. As comparison between water and hybrid nanofluids the skin friction in percentage wise factor as follows; $\beta = 0.5$ (decrease by 150.12%), $\beta = 1$ (decrease by 121.81%) and $\beta = 1.5$ (decrease by 104.81%). While the Nusselt number in percentage wise factor as follows; $\beta = 0.5$ (decrease by 0.05%), $\beta = 1$ (decrease by 0.51%) and $\beta = 1.5$ (decrease by 0.77%).

Table 6 and Table 7 shows that the skin friction and Nusselt number for variation value of $\alpha, \mathrm{M}, \gamma, \mathrm{Rd}, \lambda, \phi_1 \mathrm{and}\ \phi_2$ with different nanoparticles shape. From Table 6, the increasing value in α and M, the skin friction is observed to have the decrement for all the nanoparticle's shapes while the other parameters have an increment for all nanoparticles shapes. It is also indicating that the blades nanoparticles shape resulted in the highest skin friction coefficient for all parameters, followed by platelets shape, cylindrical shape, brick shape and spherical shape. For value of the $\alpha, \mathrm{M}, \phi_1 \mathrm{and}\ \phi_2$ is increase in Table 7, show the Nusselt number is inspected to have the increasing for all the nanoparticle's shapes while the other parameters which is γ, Rd and λ have a decrement for all nanoparticles shapes. It is also indicating that the blades nanoparticles shape resulted in the highest Nusselt number for all parameters, followed by platelets shape, cylindrical shape, brick shape and spherical shape.

Table 5
Variation in Skin Friction Coefficient and Nusselt Number for $\alpha, M, \gamma, Rd, \lambda, \phi_1$ and ϕ_2 with diverse values of Deborah number, β

α	M	γ	Rd	λ	ϕ_1	ϕ_2	Skin Friction			Nusselt Number		
							$\beta = 0.5$	$\beta = 1$	$\beta = 1.5$	$\beta = 0.5$	$\beta = 1$	$\beta = 1.5$
0°	1	45°	1	0.02	0.1	0.1	-0.318673	-0.446867	-0.564546	-11.612540	-11.630203	-11.64855
45°							-0.428399	-0.573088	-0.705058	-11.550067	-11.575786	-11.59982
70°							-0.505711	-0.662045	-0.804218	-11.505920	-11.537300	-11.56528
90°							-0.528340	-0.688079	-0.833246	-11.492976	-11.526016	-11.55515
90°	0	45°	1	0.02	0.1	0.1	-0.318673	-0.446867	-0.564546	-11.612540	-11.630203	-11.64855
	0.5						-0.428399	-0.573088	-0.705058	-11.550067	-11.575786	-11.59982
	1						-0.528340	-0.688079	-0.833246	-11.492976	-11.526016	-11.55515
	2						-0.706758	-0.893201	-1.061952	-11.390666	-11.436889	-11.47509
90°	1	0°	1	0.02	0.1	0.1	-0.512928	-0.695851	-0.864171	-11.444933	-11.474039	-11.50235
		45°					-0.528340	-0.688079	-0.833246	-11.492976	-11.526016	-11.55515
		70°					-0.484200	-0.600895	-0.705394	-11.595637	-11.629228	-11.65574
		90°					-0.157497	-0.208967	-0.260508	-11.868123	-11.867749	-11.86724
90°	1	45°	0	0.02	0.1	0.1	-0.662270	-0.828222	-0.977046	-8.727314	-8.753166	-8.77396
			1				-0.528340	-0.688079	-0.833246	-11.492976	-11.526016	-11.5552
			1.5				-0.427787	-0.581408	-0.722848	-11.626510	-11.655841	-11.68450
90°	1	45°	1	0	0.1	0.1	-1.122449	-1.296137	-1.449161	-11.285910	-11.378280	-11.441017
				0.02			-0.528340	-0.688079	-0.833246	-11.492976	-11.526016	-11.555153
				0.04			0.042400	-0.097579	-0.231411	-11.675136	-11.659847	-11.660538
90°	1	45°	1	0.02	0	0	-1.453623	-1.678830	-1.877223	-9.921381	-9.995816	-10.046429
					0.05	0.05	-0.879117	-1.071805	-1.244254	-10.609216	-10.658681	-10.696336
					0.1	0.1	-0.581174	-0.756887	-0.916571	-9.916420	-9.944928	-9.970068

Table 6
Variation in Skin Friction Coefficient for $\alpha, M, \gamma, Rd, \lambda, \phi_1$ and ϕ_2 with different nanoparticles shape

α	M	γ	Rd	λ	ϕ_1	ϕ_2	Skin Friction			
							Spherical $m = 3$	Bricks $m = 3.7$	Cylindrical $m = 4.9$	Platelets $m = 5.7$
0°	1	45°	1	0.02	0.1	0.1	-0.564546	-0.546422	-0.515490	-0.495107
45°							-0.705058	-0.686955	-0.656067	-0.635718
70°							-0.804218	-0.786146	-0.755318	-0.735015
90°							-0.833246	-0.815186	-0.784380	-0.764092
90°	0	45°	1	0.02	0.1	0.1	-0.564546	-0.546422	-0.515490	-0.495107
	0.5						-0.705058	-0.686955	-0.656067	-0.635718
	1						-0.833246	-0.815186	-0.784380	-0.764092
	2						-1.061952	-1.044015	-1.013441	-0.993322
90°	1	0°	1	0.02	0.1	0.1	-0.864171	-0.839537	-0.797612	-0.770071
		45°					-0.833246	-0.815186	-0.784380	-0.764092
		70°					-0.705394	-0.696195	-0.680449	-0.670046
		90°					-0.260508	-0.260508	-0.260508	-0.260508
90°	1	45°	0	0.02	0.1	0.1	-0.977046	-0.952375	-0.911480	-0.885239
			1				-0.833246	-0.815186	-0.784380	-0.764092
			1.5				-0.722848	-0.708228	-0.682975	-0.666144
90°	1	45°	1	0	0.1	0.1	-1.449161	-1.449161	-1.449161	-1.449161
				0.02			-0.833246	-0.815186	-0.784380	-0.764092
				0.04			-0.231411	-0.196524	-0.137163	-0.098176
90°	1	45°	1	0.02	0	0	-1.877223	-1.877223	-1.877223	-1.877223
					0.05	0.05	-1.244254	-1.238019	-1.227343	-1.220254
					0.1	0.1	-0.916571	-0.896704	-0.862818	-0.840501

Table 7
Variation in Nusselt Number Coefficient for $\alpha, M, \gamma, Rd, \lambda, \phi_1$ and ϕ_2 with different nanoparticles shape

α	M	γ	Rd	λ	ϕ_1	ϕ_2	Nusselt Number			
							Spherical $m = 3$	Bricks $m = 3.7$	Cylindrical $m = 4.9$	Platelets $m = 5.7$
0°	1	45°	1	0.02	0.1	0.1	-11.648554	-11.284426	-10.708463	-10.357145
45°							-11.599824	-11.235803	-10.660034	-10.308850
70°							-11.565283	-11.201330	-10.625683	-10.274583
90°							-11.555153	-11.191218	-10.615604	-10.264529
90°	0	45°	1	0.02	0.1	0.1	-11.648554	-11.284426	-10.708463	-10.357145
	0.5						-11.599824	-11.235803	-10.660034	-10.308850
	1						-11.555153	-11.191218	-10.615604	-10.264529
	2						-11.475096	-11.111294	-10.535920	-10.185013
90°	1	0°	1	0.02	0.1	0.1	-11.502357	-11.139799	-10.566525	-10.216988
		45°					-11.555153	-11.191218	-10.615604	-10.264529
		70°					-11.655742	-11.290021	-10.711341	-10.358240
		90°					-11.867237	-11.499730	-10.917989	-10.562856
90°	1	45°	0	0.02	0.1	0.1	-8.773961	-8.305392	-7.622874	-7.236680
			1				-11.555153	-11.191218	-10.615604	-10.264529
			1.5				-11.684496	-11.423622	-10.996154	-10.726336
90°	1	45°	1	0	0.1	0.1	-11.441017	-11.073371	-10.491392	-10.136100
				0.02			-11.555153	-11.191218	-10.615604	-10.264529
				0.04			-11.660538	-11.299493	-10.728738	-10.380811
90°	1	45°	1	0.02	0	0	-10.046429	-10.046429	-10.046429	-10.046429
					0.05	0.05	-10.696336	-10.529905	-10.255508	-10.080317
					0.1	0.1	-9.970068	-9.656056	-9.159402	-8.856486

5. Conclusions

The purpose of this study was to examine radiation and nanoparticle shape effect on aligned MHD Jeffrey hybrid nanofluids low and heat transfer over a stretching inclined plate. The nonlinear PDE is similarity transformed into a dimensionless ODE and numerically solved with the Keller Box method and MATLAB software. The effects of different factors on the velocity and temperature profiles as well as skin friction and Nusselt number were all observed. The following are the findings in this study:

i. An increase in α and M show the decrease in velocity profiles but increase in temperature profiles.
ii. An increment for γ and λ exhibit a rise in velocity profiles but decrease in temperature profiles.
iii. The increasing in radiation, Rd causes the velocity profile and temperature profile to increase.
iv. As the nanoparticle volume fraction increase, ϕ_1 and ϕ_2 the velocity and temperature profiles also increase.
v. Increasing in Deborah number, β effects the momentum boundary layer thickness is decrease for any increment of the value $\alpha, M, \gamma, Rd \text{ and } \lambda$ except for ϕ_1 and ϕ_2
vi. The skin friction coefficient increases due to $\gamma, Rd, \lambda, \phi_1$ and ϕ_2 increase except for α and M.
vii. Nusselt number is increase for an increment in α, M, ϕ_1 and ϕ_2 but decrease for $\gamma, Rd \text{ and } \lambda$.
viii. The nanoparticles shape with the highest skin friction coefficient and Nusselt number is blades followed by platelets, cylindrical, bricks and spherical shapes.

Based on the results, it has been established that blade-shaped nanoparticles in Jeffrey hybrid nanofluids significantly increase heat transfer compared to others.

Acknowledgement

The authors extend their appreciation to Universiti Teknologi MARA Shah Alam for funding this work through Geran Penyelidikan under grant number 600-RMC/GPK 5/3 (100/2020).

References

[1] Baig, Nadeem, Irshad Kammakakam, and Wail Falath. "Nanomaterials: A review of synthesis methods, properties, recent progress, and challenges." *Materials Advances* 2, no. 6 (2021): 1821-1871. https://doi.org/10.1039/D0MA00807A
[2] Choi, S. *US, and Jeffrey A. Eastman. Enhancing thermal conductivity of fluids with nanoparticles. No*. ANL/MSD/CP-84938.
[3] Setia, Hema, Ritu Gupta, and R. K. Wanchoo. "Thermophysical Properties of TiO 2-Water Based Nanofluids." In *AIP Conference Proceedings*, vol. 1393, no. 1, pp. 267-268. American Institute of Physics, 2011. https://doi.org/10.1063/1.3653712
[4] Waini, Iskandar, Anuar Ishak, and Ioan Pop. "Unsteady flow and heat transfer past a stretching/shrinking sheet in a hybrid nanofluid." *International Journal of Heat and Mass Transfer* 136 (2019): 288-297. https://doi.org/10.1016/j.ijheatmasstransfer.2019.02.101
[5] Idris, Muhammad Syafiq, Irnie Azlin Zakaria, Wan Azmi Wan Hamzah, and Wan Ahmad Najmi Wan Mohamed. "The characteristics of hybrid Al2O3: SiO2 nanofluids in cooling plate of PEMFC." *Journal of Advanced Research in Fluid Mechanics and Thermal Sciences* 88, no. 3 (2021): 96-109. https://doi.org/10.37934/arfmts.88.3.96109
[6] Khan, Muhammad Naveed, Nevzat Akkurt, N. Ameer Ahammad, Shafiq Ahmad, Abdelfattah Amari, Sayed M. Eldin, and Amjad Ali Pasha. "Irreversibility analysis of Ellis hybrid nanofluid with surface catalyzed reaction and multiple slip effects on a horizontal porous stretching cylinder." *Arabian Journal of Chemistry* 15, no. 12 (2022): 104326. https://doi.org/10.1016/j.arabjc.2022.104326

[7] Pasha, Amjad Ali, Nazrul Islam, Wasim Jamshed, Mohammad Irfan Alam, Abdul Gani Abdul Jameel, Khalid A. Juhany, and Radi Alsulami. "Statistical analysis of viscous hybridized nanofluid flowing via Galerkin finite element technique." *International Communications in Heat and Mass Transfer* 137 (2022): 106244. https://doi.org/10.1016/j.icheatmasstransfer.2022.106244

[8] Gaffar, S. Abdul, V. Ramachandra Prasad, and E. Keshava Reddy. "Computational study of Jeffrey's non-Newtonian fluid past a semi-infinite vertical plate with thermal radiation and heat generation/absorption." *Ain Shams Engineering Journal* 8, no. 2 (2017): 277-294. https://doi.org/10.1016/j.asej.2016.09.003

[9] Zokri, Syazwani Mohd, Nur Syamilah Arifin, Muhammad Khairul Anuar Mohamed, Mohd Zuki Salleh, Abdul Rahman Mohd Kasim, and Nurul Farahain Mohammad. "Influence of radiation and viscous dissipation on magnetohydrodynamic Jeffrey fluid over a stretching sheet with convective boundary conditions." *Malaysian Journal of Fundamental and Applied Sciences* 13, no. 3 (2017): 279-284.

[10] Rawi, Noraihan Afiqah, Mohd Rijal Ilias, Lim Yeou Jiann, Zaiton Mat Isa, and Sharidan Shafie. "The effect of copper nanoparticles on mixed convection flow of jeffrey fluid induced by g-jitter." *Journal of Nanofluids* 7, no. 1 (2018): 156-162. https://doi.org/10.1166/jon.2018.1433

[11] Shahzad, Faisal, Wasim Jamshed, Kottakkaran Sooppy Nisar, M. Motawi Khashan, and Abdel-Haleem Abdel-Aty. "Computational analysis of Ohmic and viscous dissipation effects on MHD heat transfer flow of Cu-PVA Jeffrey nanofluid through a stretchable surface." *Case Studies in Thermal Engineering* 26 (2021): 101148. https://doi.org/10.1016/j.csite.2021.101148

[12] Ali, Aamir, S. Saleem, Sana Mumraiz, Anber Saleem, M. Awais, and D. N. Khan Marwat. "Investigation on TiO 2–Cu/H 2 O hybrid nanofluid with slip conditions in MHD peristaltic flow of Jeffrey material." *Journal of Thermal Analysis and Calorimetry* 143 (2021): 1985-1996. https://doi.org/10.1007/s10973-020-09648-1

[13] Alqarni, Awatif J., R. E. Abo-Elkhair, Essam M. Elsaid, Abdel-Haleem Abdel-Aty, and Mohamed S. Abdel-wahed. "Effect of magnetic force and moderate Reynolds number on MHD Jeffrey hybrid nanofluid through peristaltic channel: application of cancer treatment." *The European Physical Journal Plus* 138, no. 2 (2023): 1-30. https://doi.org/10.1140/epjp/s13360-023-03689-9

[14] Jafar, Ahmad Banji, Sharidan Shafie, Imran Ullah, Rabia Safdar, Wasim Jamshed, Amjad Ali Pasha, Mustafa Mutiur Rahman et al. "Mixed convection flow of an electrically conducting viscoelastic fluid past a vertical nonlinearly stretching sheet." *Scientific Reports* 12, no. 1 (2022): 14679. https://doi.org/10.1038/s41598-022-18761-0

[15] Ilias, Mohd Rijal, Nur Sa'aidah Ismail, Nurul Hidayah AbRaji, Noraihan Afiqah Rawi, and Sharidan Shafie. "Unsteady aligned MHD boundary layer flow and heat transfer of a magnetic nanofluids past an inclined plate." *International Journal of Mechanical Engineering and Robotics Research* 9, no. 2 (2020): 197-206. https://doi.org/10.18178/ijmerr.9.2.197-206

[16] Nayan, Asmahani, Nur Izzatie Farhana Ahmad Fauzan, Mohd Rijal Ilias, Shahida Farhan Zakaria, and Noor Hafizah Zainal Aznam. "Aligned Magnetohydrodynamics (MHD) Flow of Hybrid Nanofluid Over a Vertical Plate Through Porous Medium." *Journal of Advanced Research in Fluid Mechanics and Thermal Sciences* 92, no. 1 (2022): 51-64. https://doi.org/10.37934/arfmts.92.1.5164

[17] Zainal, Nurul Amira, Roslinda Nazar, Kohilavani Naganthran, and Ioan Pop. "MHD mixed convection stagnation point flow of a hybrid nanofluid past a vertical flat plate with convective boundary condition." *Chinese Journal of Physics* 66 (2020): 630-644. https://doi.org/10.1016/j.cjph.2020.03.022

[18] Bosli, Fazillah, Mohd Rijal Ilias, Noor Hafizah Zainal Aznam, Siti Shuhada Ishak, Shahida Farhan Zakaria, and Amirah Hazwani Abdul Rahim. "Aligned magnetohydrodynamic effect on magnetic nanoparticle with different base fluids past a moving inclined plate." (2022). https://doi.org/10.21833/ijaas.2023.03.013

[19] Yashkun, Ubaidullah, Khairy Zaimi, Nor Ashikin Abu Bakar, Anuar Ishak, and Ioan Pop. "MHD hybrid nanofluid flow over a permeable stretching/shrinking sheet with thermal radiation effect." *International Journal of Numerical Methods for Heat & Fluid Flow* 31, no. 3 (2020): 1014-1031. https://doi.org/10.1108/HFF-02-2020-0083

[20] Mohamad, Ahmad Qushairi, Ilyas Khan, Lim Yeou Jiann, Arshad Khan, Mohd Rijal Ilias, and Sharidan Shafie. "Magnetohydrodynamic conjugate flow of casson fluid over a vertical plate embedded in a porous medium with arbitrary wall shear stress." *Journal of Nanofluids* 6, no. 1 (2017): 173-181. https://doi.org/10.1166/jon.2017.1294

[21] Ismail, M. A., N. F. Mohamad, M. R. Ilias, and S. Shafie. "MHD Effect on Unsteady Mixed Convection Boundary Layer Flow past a Circular Cylinder with Constant Wall Temperature." In *Journal of Physics: Conference Series*, vol. 890, no. 1, p. 012054. IOP Publishing, 2017. https://doi.org/10.1088/1742-6596/890/1/012054

[22] Rosaidi, Nor Alifah, Nurul Hidayah Ab Raji, Siti Nur Hidayatul Ashikin Ibrahim, and Mohd Rijal Ilias. "Aligned magnetohydrodynamics free convection flow of magnetic nanofluid over a moving vertical plate with convective boundary condition." *Journal of Advanced Research in Fluid Mechanics and Thermal Sciences* 93, no. 2 (2022): 37-49. https://doi.org/10.37934/arfmts.93.2.3749

[23] Ismail, Nur Suhaida Aznidar, Ahmad Sukri Abd Aziz, Mohd Rijal Ilias, and Siti Khuzaimah Soid. "Mhd boundary layer flow in double stratification medium." In *Journal of Physics: Conference Series*, vol. 1770, no. 1, p. 012045. IOP Publishing, 2021. https://doi.org/10.1088/1742-6596/1770/1/012045

[24] Soid, Siti Khuzaimah, Afiqah Athirah Durahman, Nur Hazirah Adilla Norzawary, Mohd Rijal Ilias, and Amirah Mohamad Sahar. "Magnetohydrodynamic of Copper-Aluminium of Oxide Hybrid Nanoparticles Containing Gyrotactic Microorganisms over a Vertical Cylinder with Suction." *Journal of Advanced Research in Applied Sciences and Engineering Technology* 28, no. 2 (2022): 222-234. https://doi.org/10.37934/araset.28.2.222234

[25] Ahmad, Sayyid Zainal Abidin Syed, Wan Azmi Wan Hamzah, Mohd Rijal Ilias, Sharidan Shafie, and Gholamhassan Najafi. "Unsteady MHD boundary layer flow and heat transfer of Ferrofluids over a horizontal flat plate with leading edge accretion." *Journal of Advanced Research in Fluid Mechanics and Thermal Sciences* 59, no. 2 (2019): 163-181.

[26] Ilias, Mohd Rijal. "Steady and Unsteady Aligned Magnetohydrodynamics Free Convection Flows of Magnetic and Non Magnetic Nanofluids along a Wedge, Vertical and Inclined Plates." *PhD diss., Universiti Teknologi Malaysia* (2018).

[27] Khashi'ie, Najiyah Safwa, Norihan Md Arifin, Ezad Hafidz Hafidzuddin, Nadihah Wahi, and Mohd Rijal Ilias. "Magnetohydrodynamics (MHD) flow and heat transfer of a doubly stratified nanofluid using Cattaneo-Christov model." *Universal Journal of Mechanical Engineering* 7, no. 4 (2019): 206-214. https://doi.org/10.13189/ujme.2019.070409

[28] Kamal, Mohamad Hidayad Ahmad, Noraihan Afiqah Rawi, Mohd Rijal Ilias, Anati Ali, and Sharidan Shafie. "Effect of thermal radiation on a three-dimensional stagnation point region in nanofluid under microgravity environment." *Universal Journal of Mechanical Engineering* 7 (2019): 272-284. https://doi.org/10.13189/ujme.2019.070504

[29] Ishak, Siti Shuhada, Nurul Nurfatihah Mazlan, Mohd Rijal Ilias, Roselah Osman, Abdul Rahman Mohd Kasim, and Nurul Farahain Mohammad. "Radiation Effects on Inclined Magnetohydrodynamics Mixed Convection Boundary Layer Flow of Hybrid Nanofluids over a Moving and Static Wedge." *Journal of Advanced Research in Applied Sciences and Engineering Technology* 28, no. 3 (2022): 68-84. https://doi.org/10.37934/araset.28.3.6884

[30] Hamrelaine, Salim, Fateh Mebarek-Oudina, and Mohamed Rafik Sari. "Analysis of MHD Jeffery Hamel flow with suction/injection by homotopy analysis method." *Journal of Advanced Research in Fluid Mechanics and Thermal Sciences* 58, no. 2 (2019): 173-186.

[31] Teh, Yuan Ying, and Adnan Ashgar. "Three dimensional MHD hybrid nanofluid Flow with rotating stretching/shrinking sheet and Joule heating." *CFD Letters* 13, no. 8 (2021): 1-19. https://doi.org/10.37934/cfdl.13.8.119

[32] Sajid, Tanveer, Wasim Jamshed, Rabia Safdar, Syed Modassir Hussain, Faisal Shahzad, Muhammad Bilal, Zulfiqar Rehman, Mustafa Mutiur Rahman, and Amjad Ali Pasha. "Features and aspects of radioactive flow and slippage velocity on rotating two-phase Prandtl nanofluid with zero mass fluxing and convective constraints." *International Communications in Heat and Mass Transfer* 136 (2022): 106180. https://doi.org/10.1016/j.icheatmasstransfer.2022.106180

[33] Jamshed, Wasim, Mohamed R. Eid, Rabia Safdar, Amjad Ali Pasha, Siti Suzilliana Putri Mohamed Isa, Mohammad Adil, Zulfiqar Rehman, and Wajaree Weera. "RETRACTED ARTICLE: Solar energy optimization in solar-HVAC using Sutterby hybrid nanofluid with Smoluchowski temperature conditions: a solar thermal application." *Scientific Reports* 12, no. 1 (2022): 11484. https://doi.org/10.1038/s41598-022-15685-7

[34] Shahsavar, Amin, Kasra Moradi, Çağatay Yıldız, Peyman Farhadi, and Müslüm Arıcı. "Effect of nanoparticle shape on cooling performance of boehmite-alumina nanofluid in a helical heat sink for laminar and turbulent flow regimes." *International Journal of Mechanical Sciences* 217 (2022): 107045. https://doi.org/10.1016/j.ijmecsci.2021.107045

[35] Hemalatha, R., Peri K. Kameswaran, and P. V. S. N. Murthy. "Effect of nanoparticle shape on the mixed convective transport over a vertical cylinder in a non-Darcy porous medium." *International Communications in Heat and Mass Transfer* 133 (2022): 105962. https://doi.org/10.1016/j.icheatmasstransfer.2022.105962

[36] Khetib, Yacine, Hala M. Abo-Dief, Abdullah K. Alanazi, S. Mohammad Sajadi, Rasool Kalbasi, and Mohsen Sharifpur. "Effect of nanoparticles shape on turbulent nanofluids flow within a solar collector by using hexagonal cross-section tubes." *Sustainable Energy Technologies and Assessments* 51 (2022): 101843. https://doi.org/10.1016/j.seta.2021.101843

[37] Bataller, Rafael Cortell. "Radiation effects in the Blasius flow." *Applied Mathematics and Computation* 198, no. 1 (2008): 333-338. https://doi.org/10.1016/j.amc.2007.08.037

[38] Ishak, Anuar, Roslinda Nazar, and Ioan Pop. "Mixed convection boundary layers in the stagnation-point flow toward a stretching vertical sheet." *Meccanica* 41 (2006): 509-518. https://doi.org/10.1007/s11012-006-0009-4

[39] Ishak, Anuar, Roslinda Nazar, Norihan M. Arifin, and Ioan Pop. "Mixed convection of the stagnation-point flow towards a stretching vertical permeable sheet." *Malaysian Journal of Mathematical Sciences* 1, no. 2 (2007): 217-226.

[40] NA, TY. "Computational methods in engineering boundary value problems(Book)." *New York, Academic Press, Inc.(Mathematics in Science and Engineering.* 145 (1979).

[41] Cebeci, Tuncer, and Peter Bradshaw. *Physical and computational aspects of convective heat transfer*. Springer Science & Business Media, 2012.

[42] Das, S., R. N. Jana, and O. D. Makinde. "Magnetohydrodynamic mixed convective slip flow over an inclined porous plate with viscous dissipation and Joule heating." *Alexandria Engineering Journal* 54, no. 2 (2015): 251-261. https://doi.org/10.1016/j.aej.2015.03.003

[43] Ulgen, Onur, and Timothy Thomasma. "Graphical simulation using Smalltalk-80." *SAE transactions* (1987): 1473-1482. https://doi.org/10.4271/870931